JOURNAL OF MATERIALS SCIENCE **34** (1999) 4551–4561

Structural characterization of grain pattern diversity in parametric space

TAO HUANG, TOMOHIRO TSUJI, M. R. KAMAL*, A. D. REY
Department of Chemical Engineering, McGill University,
3610 University Street, Montreal, Quebec, Canada, H3A 2B2
E-mail: kamal@chemeng.lan.mcgill.ca

Grain patterns are characterized by size and shape diversity as reflected by variations in the values of structural parameters ascribed to them. Analysis of the population of grains calls for a global analysis of all the pertinent structural parameters taken together. In this study, algorithms were developed for advanced grain image analysis, unbiased grain size-side measurement and full grain pattern recognition. The correlations of these normalized structural parameters were studied for each topological class and geometrical group, for the grain patterns formed under different nucleation-growth conditions. Relationships between the structural parameters and the grain spatial coordinates are given. This provides a useful approach to investigate the structural inhomogeneity in grain patterns. The results show strong interdependence between the topology, geometry and physical dynamics of the spherulitic grain size-shape arrangement in semi-crystalline polymeric films.

1. Introduction

Polymer systems display a variety of high-order structural features. The most common microstructure of semi-crystallines polymer is the spherulitic grain pattern. These high-order structures are closely related to their physical properties, such as optical, electrical and mechanical properties. In terms of the optical properties, for example, the grain sizes, shapes, textures, ellipsoid orientation and the inhomogeneity or diversity in those parameters have a great impact on transparency, haze and clarity of the polymer thin films. In food packaging application, the microstructural parameters also strongly influence the strength, toughness and permeability of the plastics products. In general, small grains and uniformity in the structural parameters are desirable for good mechanical properties of plastic products.

The microstructural characterization of the spherulitic grain patterns involves the full description of the physical dynamics of polymer pattern formation, the topological organization, and the geometrical arrangement. Polymer spherulitic grains are aggregates of a large number of grains of various sizes and of different shapes. This is reflected by distribution functions of the topological and geometrical parameters, such as the area of grains, $f(A)$, the perimeter, $f(P)$, and number of sides, $f(n)$ [1, 2]. In previous works [1, 3], we reported on the experimental characterization of the topological organization of highly disordered polygrains in planar films of a common model polymer, isotactic polypropylene, formed during free solidification. The topological aspects of the spherulitic grains are subjected to a comprehensive analysis, using the characterization methodology commonly employed in studies of random cellular patterns. A distinguishing feature of polymer grain patterns is the presence of topological defects. These topological defects are the mixed configurations of vertices containing 3, 4, 5, and 6 connectives, and a fraction of trivalent vertices smaller than 1. It is found that (i) the two-cell correlation functions $M_k(n)$ (the average number of k-sided grains adjoining an n-sided one) are clearly highly non-linear with n; (ii) that the common practice of plotting $nm(n)$ vs. n can conceal the non-linearity of the experimental data, where $m(n)$ is the average sum of the number of sides of the grains immediately adjacent to an n-sided grain; (iii) that the plot of the relation of average area of grains to the number of sides is non-linear and S-shaped, due to the polydisperse grain packing. These topological characteristics indicate that the polymer grain boundary network (GBN) does not follow either the mathematical Voronoi diagram or the common random cellular structures displayed by many physical systems. Thermal activation experiments show that the polymer grain pattern is a topological unstable structure with very slow dynamics. These experimental observations have been explained in relation to specific polymeric features [1].

The major efforts on studies of grain microstructures have emphasized the experimental measurement of the statistical distribution of geometrical parameters individually and the relation between the grain size, grain

* Author to whom all correspondence should be addressed.

texture and mechanical properties. In terms of material physics, the main difference between most of the material grain pattern systems and topological models lies in the explicit consideration of grain area, grain perimeter, and the number of sides of the grains. These three variables cannot be trivially decoupled. Purely topological models do not incorporate the competition between topology, geometry, and growth dynamics, and seems not to be suitable to fully characterize the material grain structures.

The grains are characterized by a diversity in their sizes and shapes as reflected by variations in the values of parameters ascribed to the grains [4]. A characteristic of this situation is that the parameters, a number of which describe the shape of grains, should not be analyzed separately. Analysis of the population of grains calls for a global analysis of all the pertinent geometrical parameters taken together. The cluster analysis method [8] helps to identify clusters (groups, or subpopulations) in the sets representing the elements studied in the space of the geometrical parameters and gives an opportunity to evaluate the effectiveness of the division into the clusters.

In this paper, we present advanced grain image analysis, unbiased grain size-side measurement and fully grain pattern recognition in Section 2. In Section 3, we focus on the cluster statistical analysis, grain sub-population grouping and inhomogeneity, developed here in multi-dimensional space of the following geometrical parameters: $\{A, P, R, C, S, E, n, x, y\}$, where A is grain area, P is perimeter, R is Feret radius (equivalent grain radius), C is chord of the grain, $S = 4\pi \times A/P^2$, is grain shape factor, $E = \tan(\theta)$, is the major axis slope of the grain interior ellipsoid, n is number of grain sides, and (x, y) is the gravity center of the grain. The experimental results and discussions are presented in Section 4.

2. Experimental sampling and image analysis

Experiments were carried out with isotatic polyporpylene (iPP, molecular weight $M_\eta = 250{,}000$). A polymer thin film was formed between two glass slides, while pressing the top slide to form a 10 μm thick polymer film. A Leitz polarizing microscope, equipped with a Leitz hot stage for polymer film solidification, was used in the direct observation experiments. JAVA-Jandel Scientific's video image system was directly connected to the microscope via a CCD camera. The pre-treatments of basic image processing were performed by using Visilog (©Noesis Vision Inc., Quebec).

Microstructure of materials is studied experimentally using various methods of imaging to resolve specific microstructural elements. In all cases, attention is focused on images of the microstructure and these are found to be of considerable complexity. More precisely, images from the material microstructure are distinguished by: (a) geometrical complexity and complicated shapes, which differ in their spatial dimensions; (b) diversity in size and shapes, which can only be properly described if a proper statistical methodology is available; (c) the presence of specific errors caused by imperfections in the imaging techniques. The characterization of microstructure usually requires an analysis

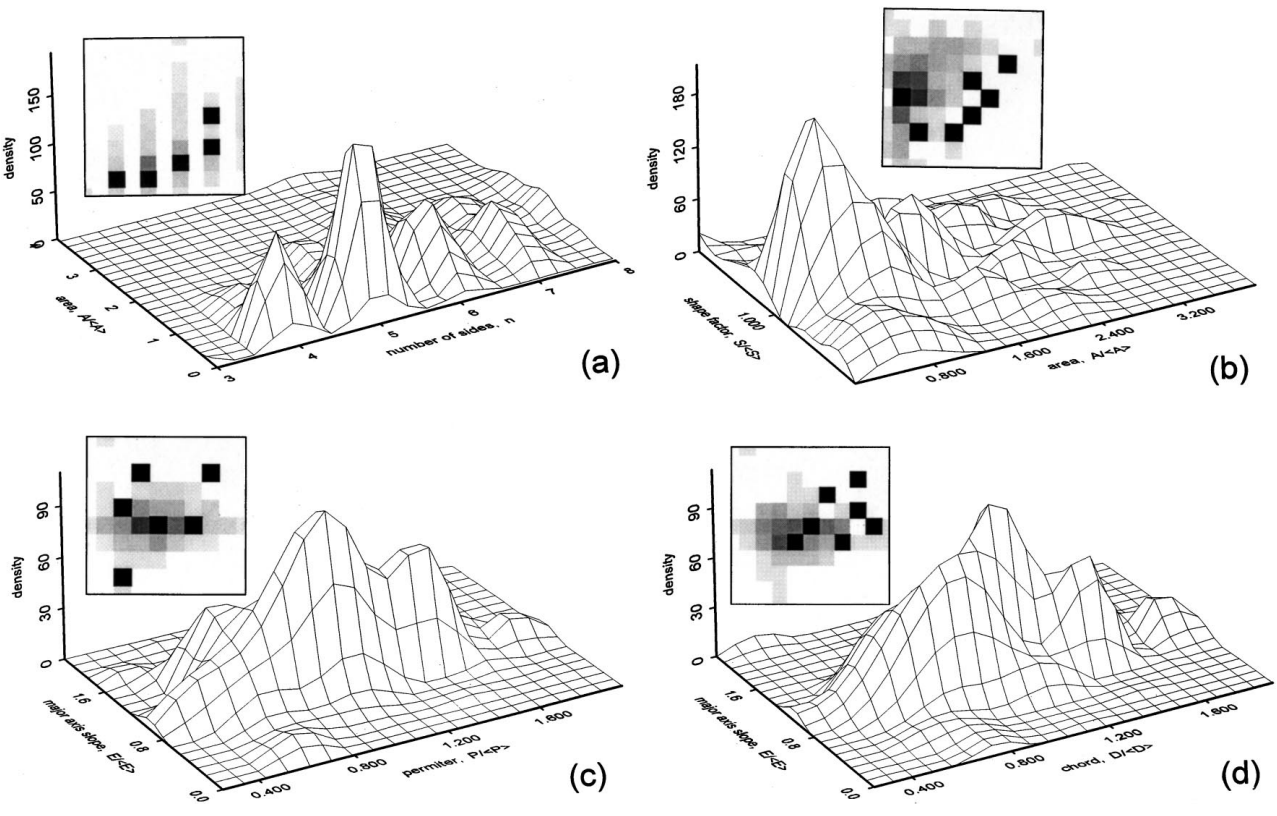

Figure 1 Typical examples of the density profiles of 2D grouping for an experimental grain pattern, and the insert images show the number of obtained groups for different geometrical parameters grouping space: (a) shows that there are 5 groups found for area vs. number of sides ($\alpha \sim n$) space; (b) shows that there are 7 groups for shape factor vs. area ($\vartheta \sim \alpha$) space; (c) shows that there are 6 groups for major axis slope vs. perimeter ($\varepsilon \sim \beta$) space; (d) shows that there are 7 groups for major axis slope vs. chord ($\varepsilon \sim \zeta$) space.

of a large number of complicated images with each of them containing the microstructural elements required.

The grain sizing is intended to compute grain size numbers and provide distributions of measurements for individual grains. The initial images are pre-processed and enhanced in order to extract grain boundaries. The techniques used are based on Watershed, Geodesic, Reconstruction, Classification and Auto-labeling algorithms [7]. Once a satisfactory grain boundary image is obtained, it is possible to edit boundaries interactively if necessary. The next step is to discard all grains that intersect with the edge of the image frame. These grains would provide inaccurate results if considered. The statistical bias due to edge effects has been corrected by using Miles-Lantuejoul approach, which was proposed by Miles [5] and illustrated by Lantuejoul [6]. Finally, the geometrical measurements can be performed automatically.

The grain siding is intended to compute grain sides from digitized images of grains and provide grain sides distribution, two-grain correlation and grain shell structure. The digital image analysis is basically the same as grain sizing. Skeletonization and Watershed detection using an arrowing technique can be used in neighbour analysis [6].

Grain spatial variability is studied by using the pair correlation function to characterize the frequency of inter-grain center distances. Populations of grains can be represented by a set of elements in a multi-dimensional geometrical space of parameters. Geometrical parameters of grain populations show an inhomogeneous character reflected by a variation in the density of elements in the parameter space. In order to characterize the geometry of grains, we apply the basic idea of cluster analysis and develop it to the characterization of polymer spherulitic grain pattern in multi-dimensional geometrical space. Thus, we consider a population of polymer spherulitic grains with each of them being described by the multi-dimensional space of the following geometrical parameters: $\{A, P, R, C, S, E, n, x, y\}$.

3. Grouping in multiple dimensional structural parametric space

Populations of grains can be represented by a set of elements in a multi-dimensional geometrical space of parameters. Geometrical parameters of grain populations show an inhomogeneous character reflected by a variation in the density of elements in the parameter space. In order to characterize the geometry of grains, we applied the basic idea of cluster analysis proposed by Kurzydlowski *et al*. [8] and extended it to the characterization of polymer spherulitic grain pattern in multi-dimensional geometrical space.

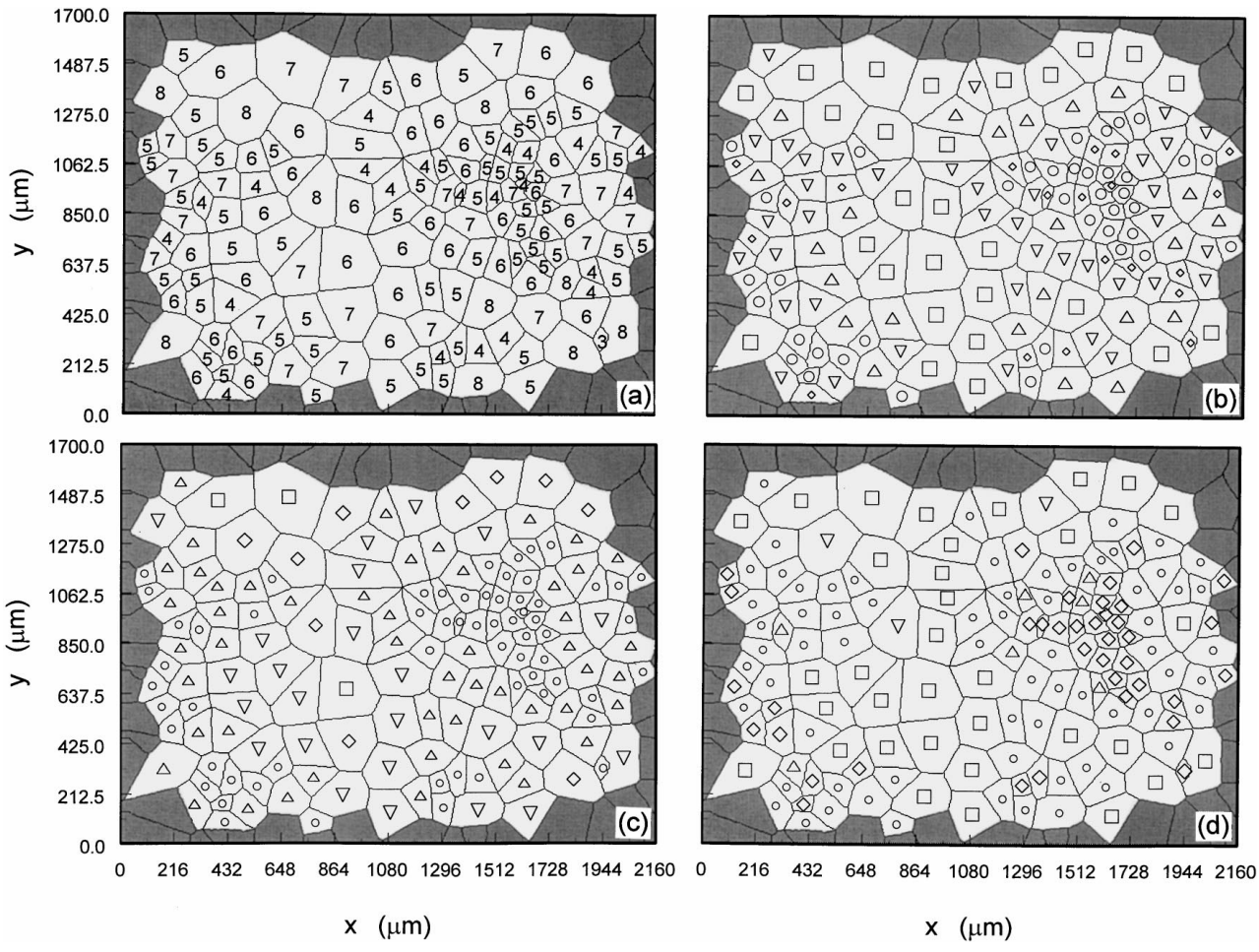

Figure 2 Typical results from grain grouping image analysis of 2D geometrical perimeters grouping for a simultaneous nucleation experiment in isothermal crystallization at $T_c = 140\,^{\circ}\mathrm{C}$: (a) the automatic grain sides labeling; (b) the grouping result in grain area and grain sides space; (c) the result in grain area and grain shape factor space; (d) the result in grain perimeter and the grain major axis slope space.

Consider a population of polymer spherulitic grains with each of them being described by the parameters: $\{A, P, R, C, S, E, n\}$. The observed values of the parameters of the first grain are marked by the subscript 1, the second grain by the subscript 2, and the values of the parameters of the grain k are marked by the subscript k. The description of the population of grains is given in the form of a matrix $\{\mathbf{G_{ij}}\}$:

$$\mathbf{G_{ij}} = \begin{pmatrix} A_1 & P_1 & R_1 & C_1 & E_1 & S_1 & n_1 \\ A_2 & P_2 & R_2 & C_2 & E_2 & S_2 & n_2 \\ \cdots & \cdots & \cdots & \cdots & \cdots & \cdots & \cdots \\ A_k & P_k & R_k & C_k & E_k & S_k & n_k \end{pmatrix} \quad (1)$$

Because the parameters in matrix $\{\mathbf{G_{ij}}\}$ have different physical meaning, they have different units. In order to avoid complication, the parameters can be normalized with respect to the mean values of the parameters to make the matrix dimensionless. The description of the population of grains is given in multi-dimensional geometrical space: $\{\alpha, \beta, \gamma, \zeta, \varepsilon, \vartheta, n\}$ and the matrix is

$$\mathbf{G_{ij}} = \begin{pmatrix} \alpha_1 & \beta_1 & \gamma_1 & \zeta_1 & \varepsilon_1 & \vartheta_1 & n_1 \\ \alpha_2 & \beta_2 & \gamma_2 & \zeta_2 & \varepsilon_2 & \vartheta_2 & n_2 \\ \cdots & \cdots & \cdots & \cdots & \cdots & \cdots & \cdots \\ \alpha_k & \beta_k & \gamma_k & \zeta_k & \varepsilon_k & \vartheta_k & n_k \end{pmatrix} \quad (2)$$

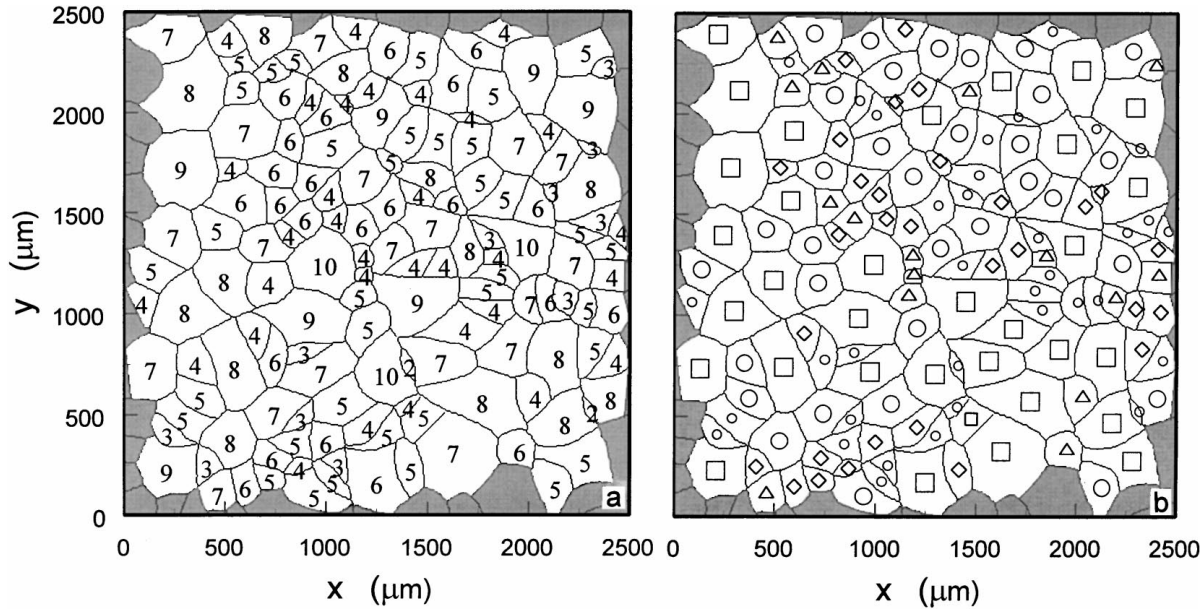

Figure 3 Typical results from grain grouping image analysis of 2D geometrical perimeters grouping for a grain image of a sequential nucleation experiment in isothermal crystallization at $T_c = 134\,^{\circ}\mathrm{C}$: (a) the automatic grain sides labeling; (b) the grouping result in grain area and grain sides space.

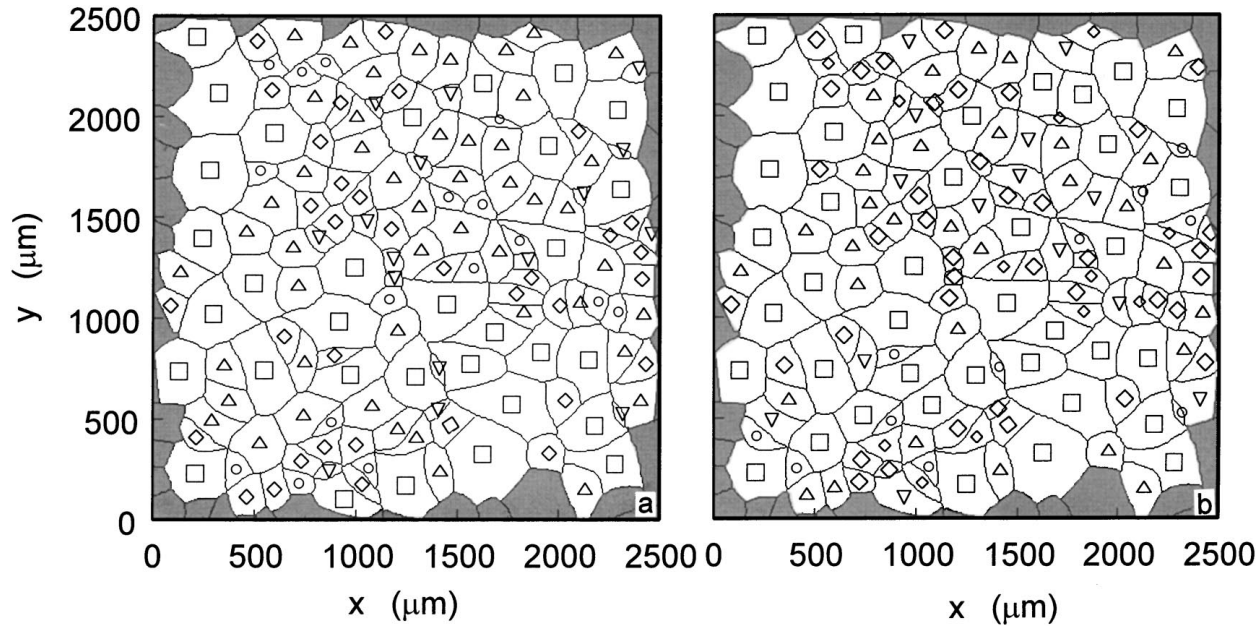

Figure 4 Typical results from grain grouping image analysis of 3D geometrical perimeters grouping for a grain image of a sequential nucleation experiment in isothermal crystallization at $T_c = 134\,^{\circ}\mathrm{C}$: (a) the result in the grain area A, the number of side grain n and the grain shape factor S; (b) the result in the grain perimeter P, the chord C and the grain major axis slope E.

By adopting a definition of the metric in the space of parameters, it is possible to group the elements into sub-populations that contain elements of similar parameters. One possible approach is defining the distance between the elements to divide the grain populations into distinctive groups, or sub-populations according to nearest neighbours criteria. Grains showing similar values of their features can be found and characterized by some average values common to a given cluster. In this way, the grains are categorized to be in different groups. Here, we chose Euclidean distance between the elements in the multi-dimensional geometrical space of the grain population: $\{\alpha, \beta, \gamma, \zeta, \varepsilon, \vartheta, n\}$. For any two elements x_{ik} and x_{jk} in the space, the distance D_{ij} is

$$D_{ij} = \sqrt{\sum_k (x_{ik} - x_{jk})^2} \tag{3}$$

and the distance matrix is

$$\mathbf{D} = \begin{pmatrix} 0 & D_{12} & \cdots & D_{1N} \\ D_{21} & 0 & \cdots & D_{2N} \\ \vdots & \vdots & \vdots & \vdots \\ D_{N1} & D_{N2} & \cdots & 0 \end{pmatrix} \tag{4}$$

The matrix $\mathbf{D}$ contains nonnegative elements and the main diagonal $D_{ii} = 0$ because no two identical element can be found in stochastic grain population. The results of grouping based on the nearest neighbours criteria, that is for any two elements in the cluster, the distance between them $D_{ij} < R$, where $R = \max_i \{\min_j \{D_{ij}\}\}$. The $\max_i$ and $\min_j$ refer to the maximum and minimum nonzero elements, respectively, of the elements in rows and columns of the distances matrix $\mathbf{D}$.

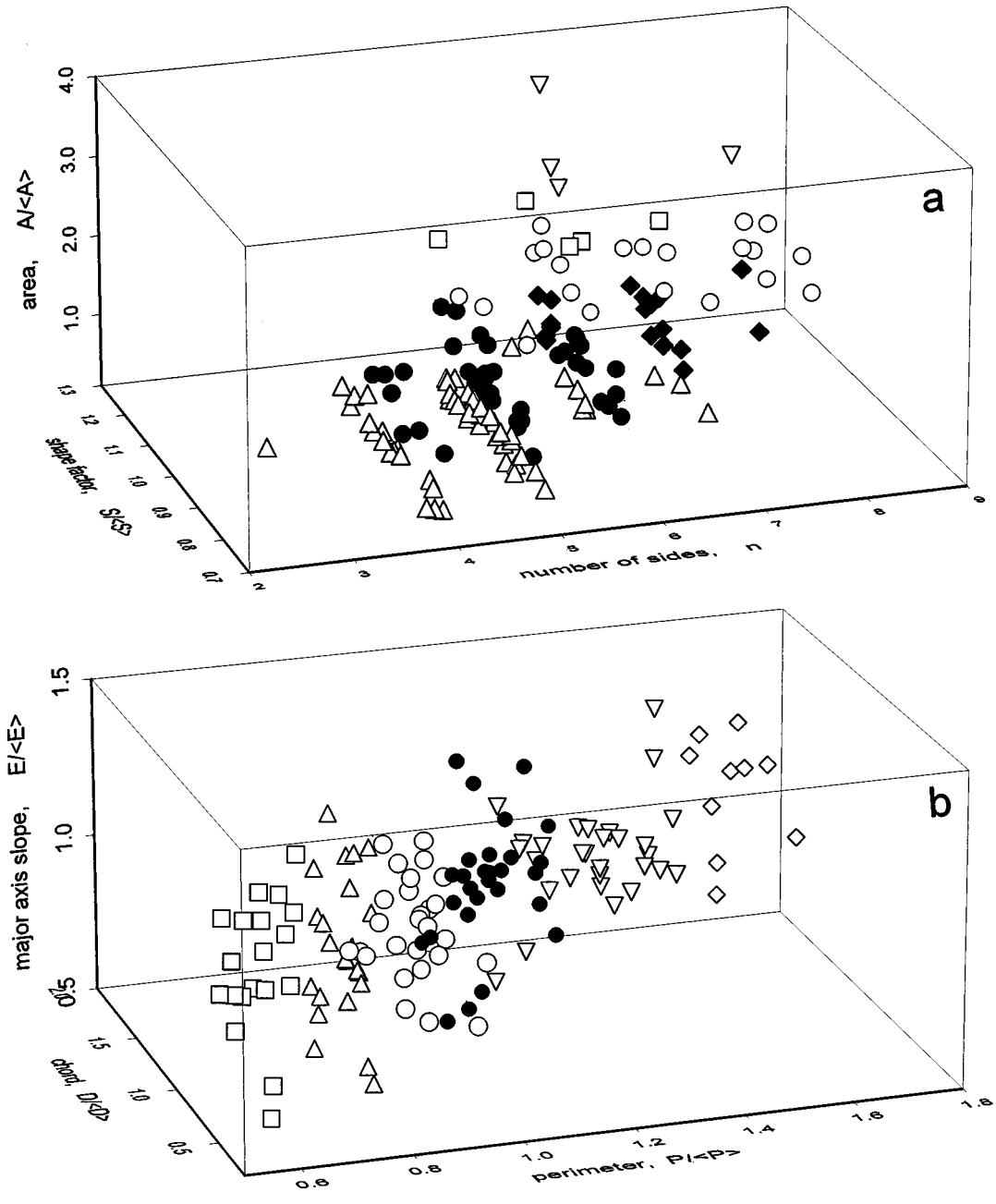

Figure 5 Grouping results for image in Fig. 2a in three-dimensional space: (a) ($\alpha \sim \vartheta \sim n$); (b) ($\beta \sim \zeta \sim \varepsilon$).

Practically, there is some uncertainty in determination of the grouping center coordinates, with the above approach. We propose a new number density profile method to correct this problem. The demonstration of the grouping is performed by firstly determining the number density profile in the structural parameter space. As an example in two dimensional parameter space $(I,\ J)$, the number density is defined as the number of data for parameters $\{I,\ J\}$. From the number density profile in the structural parameter space, the number of groups and the center of coordinates $\{I_{gk},\ J_{gk}\}$ for each group $(gk = 1, 2, \ldots, gp)$ can be easily calculated. Then, we calculate the distances $d_{k,gk}$ between element $\{I_k,\ J_k\}$ and each grouping center coordinates $\{I_{gk},\ J_{gk}\}$ for each element. We obtain a new distance matrix with dimension of $N \times gp$:

$$d_{k,gk} = \sqrt{(I_k - I_{gk})^2 - (J_k - J_{gk})^2} \qquad (5)$$

and the distance matrix is

$$d = \begin{pmatrix} d_{1,g1} & d_{1,g2} & \cdots & d_{1,gk} & \cdots & d_{1,gp} \\ d_{2,g1} & d_{2,g2} & \cdots & d_{2,gk} & \cdots & d_{2,gp} \\ \vdots & \vdots & \vdots & \vdots & \vdots & \vdots \\ d_{N,g1} & d_{N,g2} & \cdots & d_{N,gk} & \cdots & d_{N,gp} \end{pmatrix} \qquad (6)$$

By finding out the minimum distance in the row for each column, $\min_k\{d_{k,gk}\}$, we can determine to which group gk the element k belongs. Fig. 1 shows typical examples of the density profiles of 2D grouping for an experimental grain pattern, and the insert images show the number of obtained groups for different geometrical parameters in grouping space. Fig. 1a shows that there are 5 groups found for area vs. number of sides $(\alpha \sim n)$ space. Fig. 1b shows that there are 7 groups for shape factor vs. area $(\vartheta \sim \alpha)$ space. Fig. 1c shows that there

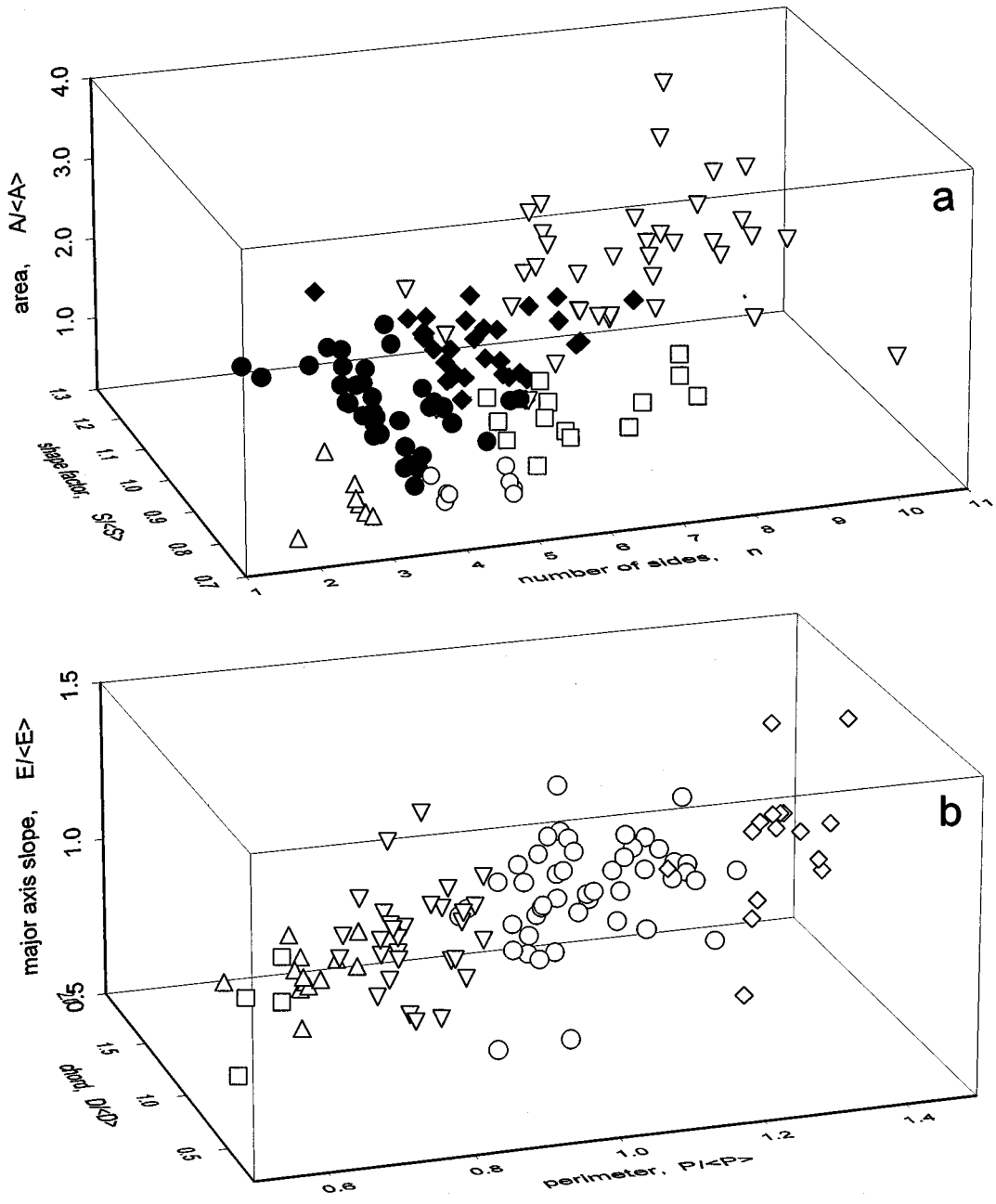

Figure 6 Grouping results for image in Fig. 3a in three-dimensional space: (a) $(\alpha \sim \vartheta \sim n)$; (b) $(\beta \sim \zeta \sim \varepsilon)$.

are 6 groups for major axis slope vs. perimeter ($\varepsilon \sim \beta$) space. Fig. 1d shows that there are 7 groups for major axis slope vs. chord ($\varepsilon \sim \zeta$) space.

4. Experimental results and discussions

4.1. Visualized grain grouping results

In order to fully provide structural recognition of the grain patterns, we built in the relationship between the structural parameters grouping and the grain spatial coordinates by associating the grouping assignment back to the grain gravity center. The examination in three-dimensional space or multiple dimensional space can be performed by using the same algorithms. As an example, Fig. 2 shows the results of the above processing for a grain image of a simultaneous nucleation experiment in isothermal crystallization at $T_c = 140\,^{\circ}\mathrm{C}$. Fig. 2a shows the result of the automatic grain sides labeling. Fig. 2b shows the visualized grouping result in grain area and grain sides space. Fig. 2c is the result in grain area and grain shape factor space. Fig. 2d is the result in grain perimeter and the grain major axis slope space. In Fig. 2, the different symbols represent the different groups. Fig. 3 shows similar results of 2D geometrical perimeters grouping for a grain image of a sequential nucleation experiment in isothermal crystallization at $T_c = 134\,^{\circ}\mathrm{C}$. Fig. 4 shows similar results of 3D geometrical perimeters grouping for a grain image of a sequential nucleation experiment in isothermal crystallization at $T_c = 134\,^{\circ}\mathrm{C}$, where (a) is the result in the grain area A, the number of sides of grain n and the grain shape factor S; (b) is the result in the grain perimeter P, the chord C and the grain major axis slope E.

4.2. Grain structural correlation in 3D parameter space

Fig. 5 shows the analysis of the groups for the image in Fig. 2a under simultaneous nucleation conditions in three-dimensional space ($\alpha \sim \vartheta \sim n$) and ($\beta \sim \zeta \sim \varepsilon$). Depending on the size of the division α, there are five groups identified in ($\alpha \sim \vartheta \sim n$) 3D space. Depending on the perimeter of the division β, there are six groups identified in ($\beta \sim \zeta \sim \varepsilon$) 3D space. The same analysis was done for the image in Fig. 3a under sequential nucleation condition in three-dimensional space ($\alpha \sim \vartheta \sim n$) and ($\beta \sim \zeta \sim \varepsilon$) as shown in Fig. 6. Two important structural features were found from the above grouping analysis:

(a) the grouping results indicate that there are some certain patterns in distribution of their structural parameters;

(b) the grouping results show that the population of grains depends upon the nucleation-growth condition or the thermal history of the grain pattern formation processes. In order to clarify this issue, we discuss plots of two parameters in the 3D grouping results in detail.

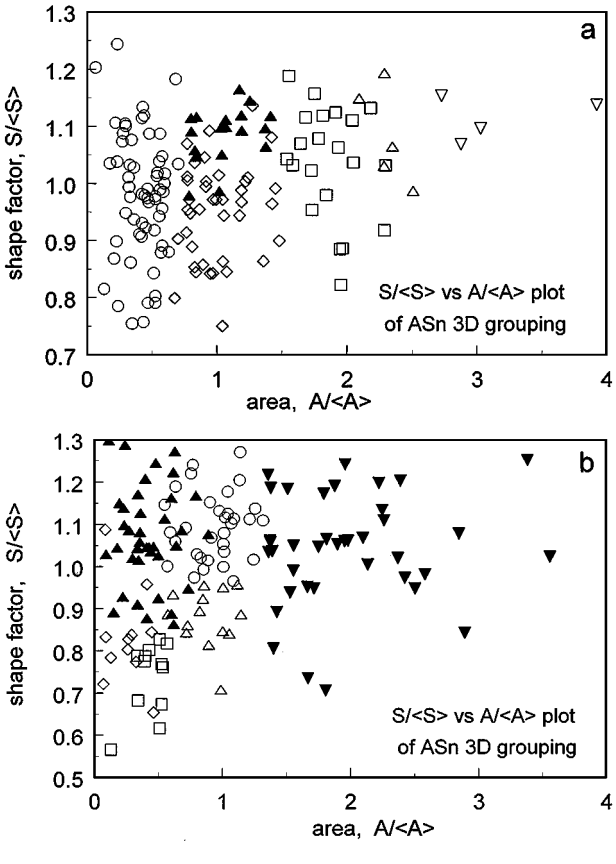

Figure 7 Relationship between normalized shape factor ϑ and its normalized grain area α of above 3D ($\alpha \sim \vartheta \sim n$) grouping: (a) grain patterns in Fig. 2a; (b) grain patterns in Fig. 3a, respectively.

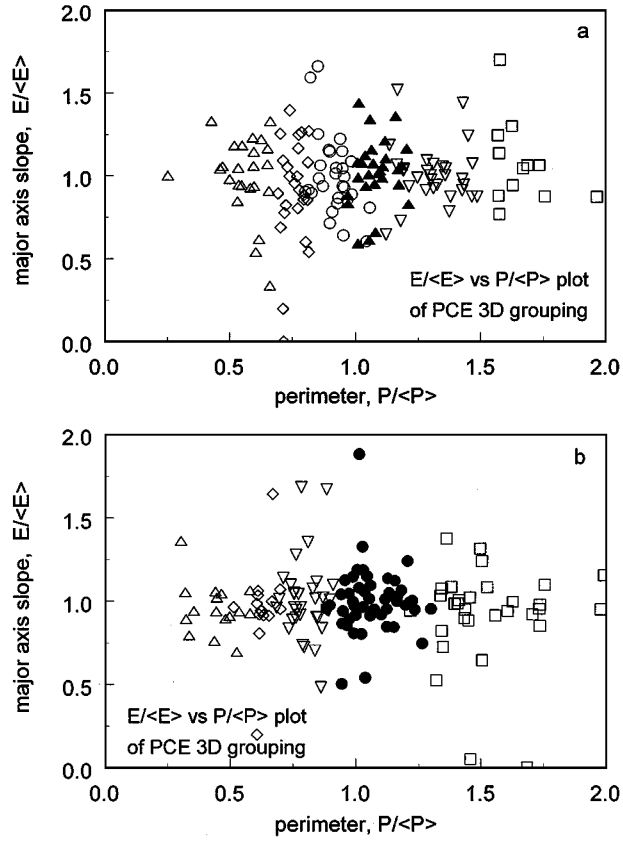

Figure 8 Relationship between normalized major axis slope of the grain interior ellipsoid ε and its normalized grain perimeter β of above 3D ($\beta \sim \zeta \sim \varepsilon$) grouping: (a) grain patterns in Fig. 2a; (b) grain patterns in Fig. 3a, respectively.

Fig. 7a and b show the relation between normalized shape factor ϑ and its normalized grain area α of the above 3D ($\alpha \sim \vartheta \sim n$) grouping for grain patterns formed under simultaneous and sequential nucleation conditions, respectively. For the simultaneous nucleation case, Fig. 7a shows that the groups detected for the smaller $\alpha < 1$ give larger variations in their shape factor ϑ, while for the larger $\alpha > 1$, they give smaller variations in their shape factor ϑ. However, for the sequential nucleation case, Fig. 7b shows that the groups detected for the smaller $\alpha < 1$ give smaller variations in their shape factor ϑ, while for the larger $\alpha > 1$, they give larger variations in their shape factor ϑ.

Fig. 8a and b show the relation between normalized major axis slope of the grain interior ellipsoid ε and its normalized grain perimeter β of the above 3D ($\beta \sim \zeta \sim \varepsilon$) grouping for grain patterns formed under simultaneous and sequential nucleation conditions, respectively. For the simultaneous nucleation case, Fig. 8a shows that ε has larger variations depending on the perimeter of the division β; However, for the sequential nucleation case, Fig. 8b shows that ε has smaller variations from $\varepsilon = 1$.

Fig. 9 shows the normalized grain area α as a function of the number of grain sides n. For both nucleation cases, grain area increased with increas ing n. This expresses the tendency for the smaller grains with less sides and larger grain with more sides. The relationship between normalized perimeter and normalized

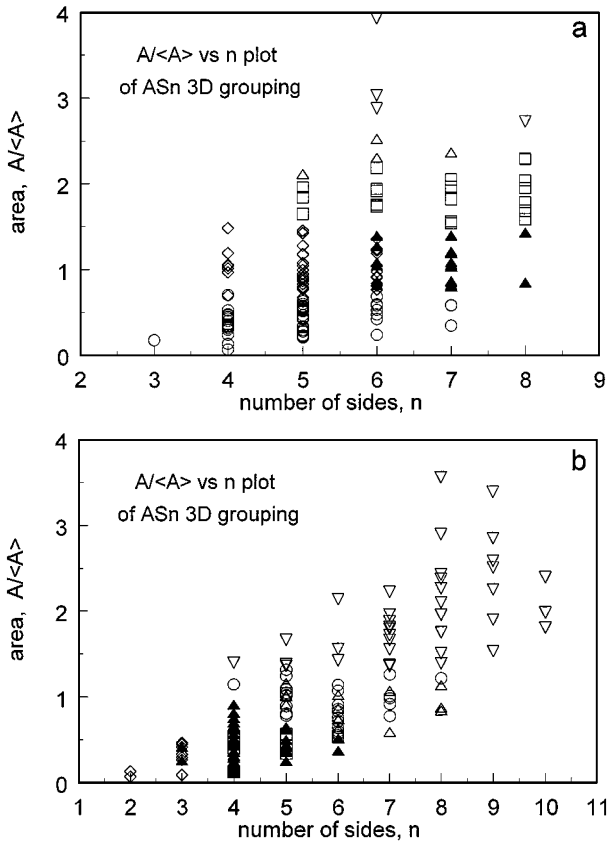

Figure 9 Normalized grain area α as the function of the number of grain sides n: (a) grain patterns in Fig. 2a; (b) grain patterns in Fig. 3a, respectively.

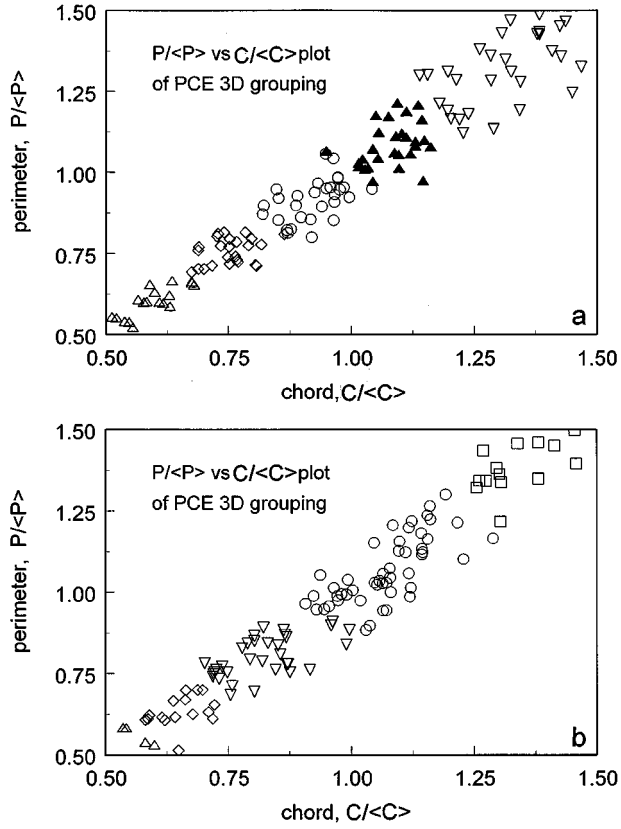

Figure 10 Relationship between normalized perimeter and normalized chord, $\beta = \zeta$: (a) grain patterns in Fig. 2a; (b) grain patterns in Fig. 3a, respectively.

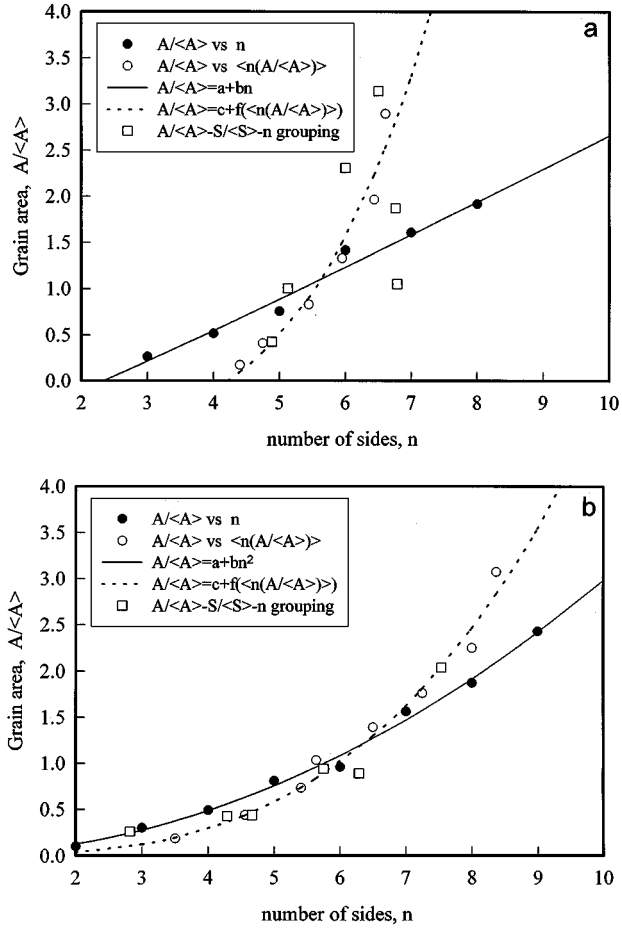

Figure 11 Two-parametric distribution function of normalized area vs. number of grain sides: (a) grain patterns from Fig. 2a; (b) grain patterns from Fig. 3a, respectively.

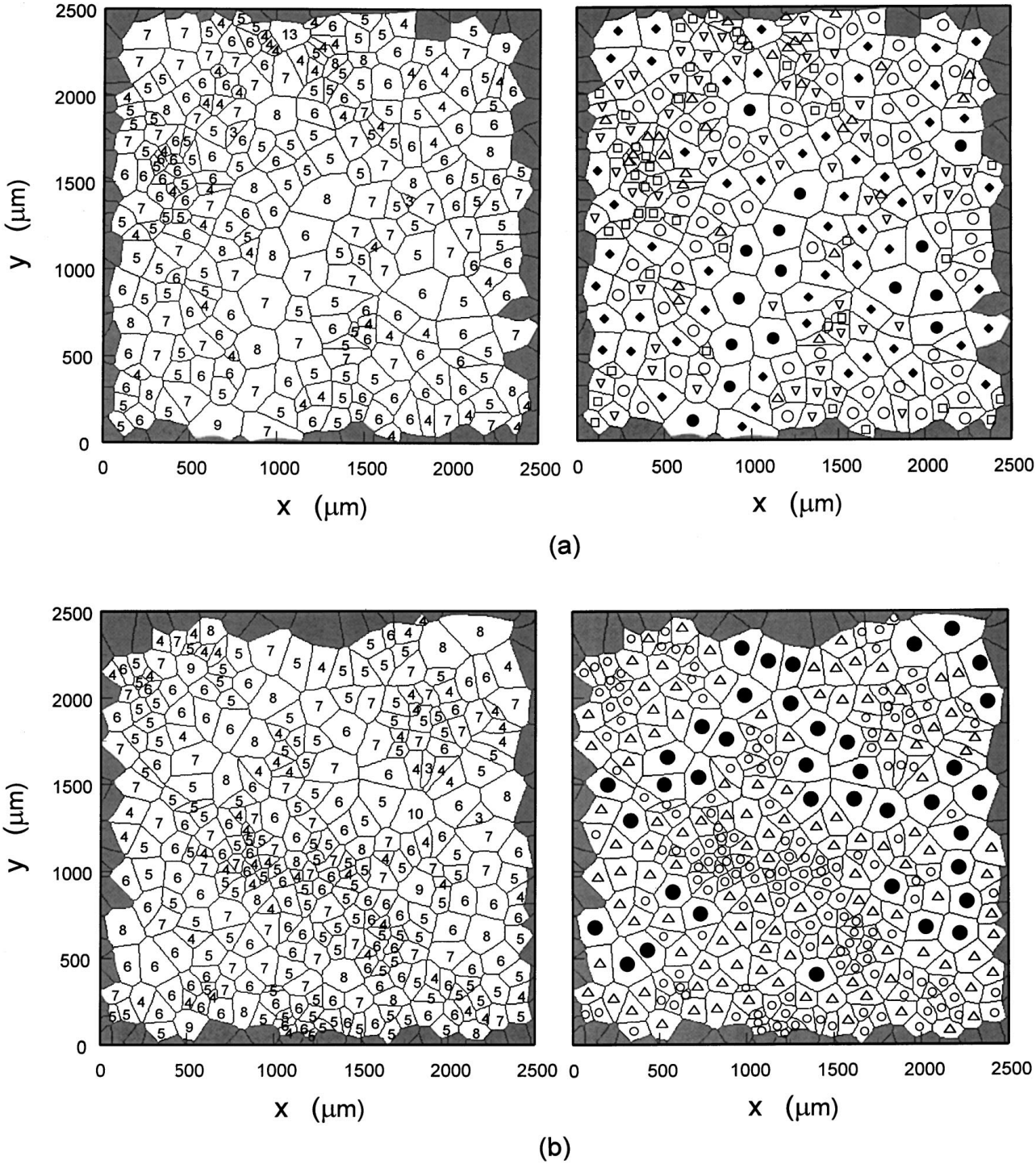

Figure 12 Visualized grain diversities of two experimental grain pattern formed at similar crystallization conditions: (a) is relatively homogeneous; (b) there is a tendency for spatial clustering.

chord, $\beta = \zeta$, was found for both nucleation cases as shown in Fig. 10.

The above results indicate that the grouping analysis quantitatively distinguished the structural differences between two main kinds of grain structures which were formed under simultaneous and sequential nucleation conditions. The grouping analysis results show that the most efficient descriptions of the grain structure are the following groupings in three-dimensional space: area/shape factor/grain sides, ($\alpha \sim \vartheta \sim n$), and perimeter/chord/grain major axis slope, ($\beta \sim \zeta \sim \varepsilon$). It also indicates that the grain area/perimeter is most important grain geometrical characteristic.

4.3. Grain size-shape correlation

For evaluating a simple geometrical description of the grain patterns, two types of grain size-shape correlations must be known [4, 9]:

(a) the average area $\langle \alpha_n(n) \rangle$ for grains of the given number of sides n, and

(b) the average number of sides $\langle n_\alpha(\alpha) \rangle$ for grains of a given normalized grain area $\langle \alpha_\alpha(n) \rangle$.

Fig. 11 shows the plot of the statistical data from experimental results of the two-parameter distribution

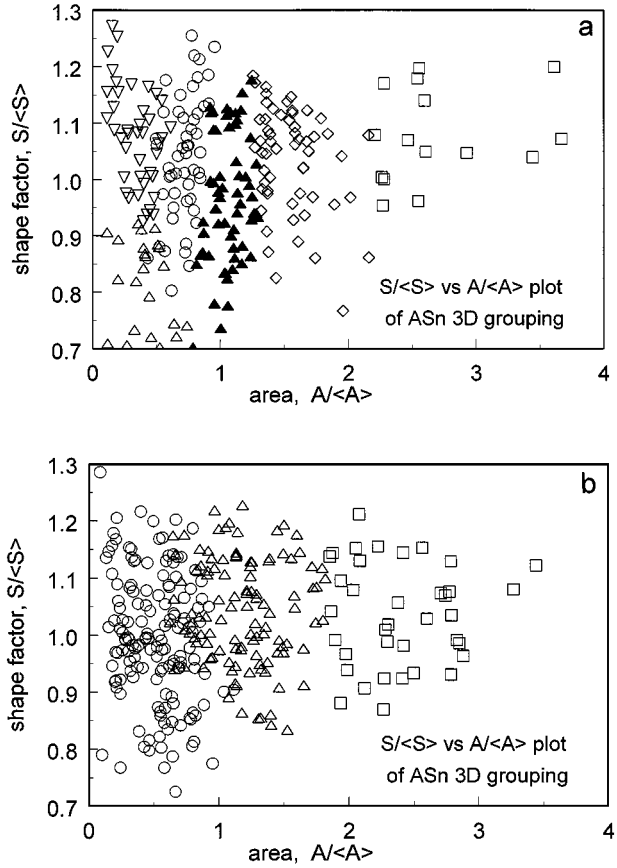

Figure 13 The area/shape factor/grain sides, ($\alpha \sim \vartheta \sim n$), 3D grouping analysis for: (a) for grain pattern in Fig. 12a; (b) for grain pattern in Fig. 12b.

function. The solid circles represent the $\langle \alpha_n(n) \rangle$ vs. n, the empty circles represent $\langle \alpha_\alpha(n) \rangle$ vs. $\langle n_\alpha(\alpha) \rangle$, and the empty squares represent the average value from the result of 3D ($\alpha \sim \vartheta \sim n$) grouping. The grouping results more or less tend to the results of $\langle \alpha_\alpha(n) \rangle$ vs. $\langle n_\alpha(\alpha) \rangle$ for both nucleation cases. This indicates that the grain area parameter is the most important grain geometrical characteristic.

Although this two-parametric distribution function cannot be expressed in a unique mathematical relationship, valid for the individual grains, statistical relationships may be obtained. The best fitting equation for the simultaneous nucleation case is

$$\langle \alpha_n(n) \rangle = a + bn \tag{7}$$

$$\langle \alpha_\alpha(n) \rangle = c + d[\langle n_\alpha(\alpha) \rangle]^4 \tag{8}$$

where $\alpha = -0.6854$, $b = 0.2719$; and $c = -0.52$, $d = 0.00183$; for the reported experimental data.

The best fitting equation for the sequential nucleation case is

$$\langle \alpha_n(n) \rangle = a + bn^2 \tag{9}$$

$$\langle \alpha_\alpha(n) \rangle = c + d[\langle n_\alpha(\alpha) \rangle]^3 \tag{10}$$

where $a = 0.004$, $b = 0.0305$; and $c = 0.0349$, $d = 0.039$; for the reported experimental date.

4.4. Inhomogeneity in grain structures

Because the structural parameters grouping can be visualized with the real grain geometrical/spatial coordinates, it becomes possible to investigate the structural inhomogeneity in grain patterns. Here, we present an example which indicates this approach. Fig. 12 shows the visualized grain diversities of two experimental grain patterns formed at similar crystallization conditions. The main difference between them is that the nuclei spatial distribution for (a) is relatively homogeneous, while for (b) there is a tendency for spatial clustering. Fig. 13 shows the results of the 3D ($\alpha \sim \vartheta \sim n$) grouping analysis. These results show that the grouping analysis can quantitatively distinguish the structural differences and the diversities of grain structures.

5. Conclusions

The grains are characterized by a diversity in their sizes and shapes, as reflected by variations in the values of structural parameters ascribed to the grains. Analysis of the population of grains calls for a global analysis of all the pertinent structural parameters taken together. In this study, algorithms have been developed for advanced grain image analysis, unbiased grain size-side measurement, and full grain pattern recognition. The correlations of these normalized structural parameters were studied for each topological class, and geometrical groups for the grain patterns formed under different nucleation-growth condition. The relationship was evaluated between the structural parameters grouping and the grain spatial coordinates. The major findings are as follows:

(1) The grouping analysis identified quantitatively the grain structural characteristics and the structural inhomogeneity or diversities in grain patterns.

(2) The evaluation shows that the most efficient descriptions of the grain structure are the groupings in three-dimensional space: area/shape factor/grain sides, ($\alpha \sim \vartheta \sim n$), and perimeter/chord/grain major axis slope, ($\beta \sim \zeta \sim \varepsilon$).

(3) The grouping analysis results indicate that the grain area/parameter is the most important grain geometrical characteristic.

(4) The two-parameter grain size-sides distribution function yields certain statistical relationships; however, it is different for different nucleation cases.

(5) The grouping analysis quantitatively distinguished the structural difference between two main kinds of grain structures which were formed under simultaneous and sequential nucleation conditions.

Acknowledgements

The authors would like to thank to Dr. J. Bystrzycki for his helpful discussion. T. H. thanks Mr. Luc Nocente and Mr. Aryé Haliooa, (Noesis Vision Inc., Quebec), who made Visilog 5.02 available for basic image processing. This work is supported by research grants from the Natural Science and Engineering Research Council

of Canada and the Ministére de l'Education, Gouvernement du Québec.

References

1. TAO HUANG, M. R. KAMAL and A. D. REY, *J. Mater. Sci. Lett.* **14** (1995) 220.
2. *Idem.*, in "Grain-size and Mechanical Properties—Fundamental and Applications," edited by M. A. Otooni *et al.* (Pittsburgh, PA, 1994) pp.193–198.
3. *Idem.*, *J. Mater. Sci*. **32** (1997) 4085.
4. *Idem.*, Material Research Society 95Fall Meeting, Boston, 1995.
5. R. E. MILES, in "Stochastic Geometry," edited by D. G. Kendall and E. F. Harding (Wiley, New York, 1974) p. 228. Springer Lecture Notes in Biomathematics (1978) Vol. 23, p. 115.
6. C. LANTUEJOUL, in "Special Issue of Practical Metallography," edited by J. L. Cherman (Riederer-Verlag, Stuttgart, 1978); Springer Lecture Notes in Biomathematics (1978) Vol. 23; Proc. NATO ASI on Digital Image Analysis, Series E (1980) No. 34, p. 107.
7. J. SERRA, "Image Analysis and Mathematical Morphology" (Academic Press, London, 1982) Vol. 1 and 2.
8. K. J. KURZYDLOWSKI, J. BYSTRZYCKI and T. CZUJKO, *Materials Characterization* **32** (1994) 105.
9. G. ABBRUZZESE, I. HECKELMAN and K. LUCKE, *Acta Matell. Mater*. **40** (1992) 2662.

Received 6 February 1998
and accepted 24 February 1999